



# Assimilation of Pseudo-Tree-Ring-Width observations into an Atmospheric General Circulation Model

Walter Acevedo<sup>1</sup>, Bijan Fallah<sup>2</sup>, Sebastian Reich<sup>1</sup>, and Ulrich Cubasch<sup>2</sup>

<sup>1</sup>Institut für Mathematik, Universität Potsdam, Karl-Liebknecht-Strasse 24-25, 14476 Potsdam, Germany.

<sup>2</sup>Institut für Meteorologie, Freie Universität Berlin, Carl-Heinrich-Becker-Weg 6-10, 12165 Berlin, Germany.

*Correspondence to:* Bijan Fallah (info@bijan-fallah.com)

**Abstract.** We investigate the assimilation of Tree-Ring-Width (TRW) chronologies into an atmospheric global climate model using Ensemble Kalman Filter (EnKF) techniques and a process-based tree-growth forward model as observation operator. Our results, within a perfect-model experiment setting, indicate that the nonlinear response of tree-growth to surface temperature and soil moisture does deteriorate the operation of the time-averaged EnKF methodology. Moreover, this skill loss appeared significantly sensitive to the structure of growth rate function, used to represent the Principle of Limiting Factor (PLF)s within the forward model. On the other hand, it was observed that the error reduction achieved by assimilating a particular pseudo-TRW chronology is modulated by the strength of the yearly internal variability of the model at the chronology site. This result might help the dendrochronology community to optimize their sampling efforts. In our experiments, the “online” (with cycling) paleo Data Assimilation (DA) approach did not outperform the “offline” (no-cycling) one, despite its considerable additional implementation complexity.

## 1 Introduction

The low-frequency temporal variability of the climate system can not be estimated from the available time span of instrumental climate records. Accordingly, paleoclimate reconstruction must necessarily rely on the usage of the so-called proxy records. These natural archives exhibit, nonetheless, several problematic features, e.g., low time-resolution, sparse and irregular spatial distribution, complex nonlinear response to climate and high noise levels. Therefore the proper extraction of the climate signal therein contained is still an open question (Evans et al., 2013).

To the present, many different paleoclimate modeling ideas have been proposed, e.g., data-driven statistical techniques, climate model hindcasts and Bayesian probabilistic methods (see Crucifix (2012) as a review). Among this plethora of approaches, DA methodologies are today particularly appealing as they allow to systematically combine the information of paleoclimate records with the dynamical consistence of climate simulations (Oke et al., 2002; Evensen, 2003; Hughes et al., 2010; Brönnimann, 2011; Bhend et al., 2012; Hakim et al., 2013; Steiger et al., 2014; Matsikaris et al., 2015; Hakim et al., 2016).

Heretofore, several very diverse paleo-DA schemes have been investigated providing very encouraging results (see (Hughes and Ammann, 2009; Widmann et al., 2010) as reference): Pattern Nudging (von Storch et al., 2000) and Forcing Singular



Vectors (Barkmeijer et al., 2003; van der Schrier and Barkmeijer, 2005) techniques were designed to curb the atmospheric circulation towards a target pattern by means of an artificial term added to the model dynamics. 4D-Var methodology has been used to assimilate pseudo-proxies into an ocean model (Paul and Schäfer-Neth, 2005; Kurahashi-Nakamura et al., 2014). EnKF was adapted to time-averaged observations (Dirren and Hakim, 2005) and tested for a hierarchy of atmospheric models (Huntley and Hakim, 2010; Bhend et al., 2012; Pendergrass et al., 2012; Steiger et al., 2014). Particle filter has been tested with an Earth system model of intermediate complexity (Annan and Hargreaves, 2012; Dubinkina and Goosse, 2013; Mathiot et al., 2013; Dubinkina et al., 2011).

A typical assumption in most of the paleo-DA studies so far conducted is that the climate-proxy relation is linear. Nonetheless, currently it is widely recognized that climate proxies are the result of complex recording processes, which can have physical, chemical and biological nature. Furthermore, several research groups have already developed and validated forward models for several proxy types (Evans et al., 2013). Hence, in order to increase the realism of DA-based climate reconstructions, it is relevant and pertinent to connect the climate state space to the proxy space by way of forward models (Acevedo et al., 2015). Following this train of thought, Acevedo et al. (2015) [AC15, hereafter] evaluated the applicability of the process-based TRW forward model Vaganov-Shashkin-Lite (VSL) (Tolwinski-Ward et al., 2011) as observation operator within a simplified DA setting. Using a chaotic 2-scale dynamical system as a toy model, AC15 generated pseudo-TRW observations and assimilated them via the Time-Averaged (TA) -EnKF algorithm (Dirren and Hakim, 2005). This paper follows closely the rationale of AC15 but now within a more realistic scenario where an Atmospheric General Circulation Model (AGCM) is used as dynamical system and the observational network resembles the currently available TRW chronologies.

The main objectives of this study are to shed light on the following four fundamental questions :

- 1) Can paleo-DA improve the skill of the model for the *forecast* (prior) state?
- 2) Can paleo-DA improve the skill of the model for the *analysis* (posterior) state?
- 3) Can an on-line (“with cycling”) DA outperform an “off-line” (“nocycling”) one (see Sec.4 for the definition of “off-line”)?
- 4) How does the nonlinear response of tree-growth to surface temperature and soil moisture affect the performance of the time-averaged EnKF-DA method?

The third question is one of the most important challenges in the field of the paleo-DA. Considering only the computational expenses of an on-line DA scheme with a realistic coupled GCM is far beyond the affordable limits of today’s computers. On the other hand, state-of-the-art climate models have little or no predictive skill on the long timescale of proxy records (Hakim et al., 2016). The fourth question, to our knowledge, has not been yet explicitly investigated in any of the paleo-DA studies.

In section 2 we describe the DA technique, the TRW forward model, the climate model as well as the experimental setting used. Our numerical results are shown in section 3, followed by a discussion in section 4.



## 2 Materials and Methods

### 2.1 Data assimilation method

Among all the available DA techniques, EnKF (Burgers et al., 1998) offers an appealing trade-off between accuracy, implemen-  
 5 of ensemble members (Whitaker et al., 2009). Its implementation does not require adjoint model and uncertainty estimates can  
 be directly obtained from the ensemble spread (Hamill, 2006). The main disadvantage of EnKF, within a paleoclimate setting,  
 is its inability to handle strongly non-Gaussian Probability Density Functions (PDFs), which can result from the nonlinearities  
 of climate models and observation operators. Nonetheless, it is very difficult to remove this limitation, given that strictly non-  
 Gaussian DA techniques have been so far prohibitively expensive to run for high dimensional systems. However, validation of  
 10 the different DA schemes in toy models or/and realistic climate models with pseudo observations or different types of proxies  
 is of particular importance (Brönnimann et al., 2013).

Following the rationale used in the experiments of AC15, pseudo-TRW observations are generated using Vaganov-Shashkin-  
 Lite (VSL) (Tolwinski-Ward et al., 2011, 2013) as observation operator. Afterward, the TA state of the atmosphere is estimated  
 via EnKF and the Time-Averaged Update (TA-Up) approach. The impact of the representation of the PLF on the filter perfor-  
 15 mance is studied using as reference of the assimilation of TA linear observations.

### 2.2 TRW Forward Model

Here, we review the forward operator's formulation which was embedded by AC15 into the framework of Fuzzy Logic (FL)  
 theory.

#### 2.2.1 VSL Model

20 The limiting factors in the VSL model for tree-ring growth are near-surface air temperature  $T$  and soil moisture  $M$ . These  
 variable influence the tree development by means of “growth response” functions  $g_T$  and  $g_M$ . Using a piece-wise linear  
 “standard ramp” function (Tolwinski-Ward et al., 2014)

$$\Psi(u) = \begin{cases} 0 & \text{if } 0 \geq u \\ u & \text{if } 0 < u \leq 1 \\ 1 & \text{if } u > 1, \end{cases}$$

VSL's growth responses at a particular time is expressed as:

$$25 \quad g_T = \Psi \left( \frac{T - T^L}{T^U - T^L} \right) \quad (1)$$

and

$$g_M = \Psi \left( \frac{M - M^L}{M^U - M^L} \right). \quad (2)$$



Where  $T^L$  and  $M^L$  denote lower thresholds below which there is no growth, while  $T^U$  and  $M^U$  present upper thresholds above which tree growth is optimal. The corresponding growth rate  $G_{MIN}$  is determined by the smallest growth response, i.e.,

$$G_{MIN} = \min\{g_T, g_M\}, \quad (3)$$

5 The yearly TRW values  $W$  are obtained as following:

$$W_n = \int_{t_n - \tau}^{t_n} G_{MIN}(t) I(t) dt. \quad (4)$$

Where  $I$  is the relative local insolation.

### 2.2.2 VSL in the framework of Fuzzy Logic

AC15 have claimed that the VSL's formulation of the PLF determines the fuzzy set of temperature-moisture conditions which optimize the tree growth. Accordingly, we have selected three different t-norms:

(i) smallest growth response or original VSL or VSL with Minimum t-norm (VSL-Min):

$$G_{MIN} = \min\{g_T, g_M\}, \quad (5)$$

(ii) product growth response or VSL with Product t-norm (VSL-Prod):

$$G_{PROD} = g_T \cdot g_M \quad (6)$$

15 (iii) temperature growth response or VSL with Temperature t-norm (VSL-T):

$$G_T = g_T \quad (7)$$

## 2.3 Experimental Setting

### 2.3.1 SPEEDY model

20 The Simplified Parametrizations, primitive-Equation Dynamics (SPEEDY) model (Molteni, 2003a) is an intermediate complexity AGCM comprising a spectral dynamical core and a set of simplified physical parametrizations, based on the same principles as state-of-the-art AGCM but tailored to work with just a few vertical levels.

25 SPEEDY's dynamical core solves the hydrostatic primitive equations by means of the spectral transform developed by Bourke (1974), which uses absolute temperature, logarithm of the surface pressure, specific humidity, divergence and vorticity as basic prognostic variables. The time stepping is performed via a leapfrog scheme with an standard Robert-Asselin filter (Robert, 1966). The sub-grid scale processes parametrized in speedy are convection, large-scale condensation, clouds, short- and long-wave radiation, surface fluxes, and vertical diffusion.



In this paper we employ the version 32 of SPEEDY, featuring seven levels in the vertical (L7) and standard Gaussian grid of 96 by 48 points in the horizontal, which correspond to a triangular spectral truncation at total wave number 30 (T30). The top and bottom layers are meant to represent the stratosphere and the planetary boundary layer, respectively. Despite of its low resolution and the relative low complexity of its parametrizations, SPEEDY still captures many observed global climate features in a realistic way, while its computational cost is at least one order of magnitude lower than the one of sophisticated state-of-the-art AGCM's at the same horizontal resolution (Molteni, 2003a). This latter virtue, makes SPEEDY specially suitable for studies involving long ensemble runs, like the ones presented in this paper.

### 2.3.2 Filter implementation

The SPEEDY model is embedded by Miyoshi (2005) into the ensemble DA framework using the Local Ensemble Transform Kalman Filter (LETKF) (Hunt et al., 2007), the so called SPEEDY-LETKF framework. The parallel FORTRAN 90 implementation of the LETKF is promising for high resolution model given that the calculation of the analysis for a particular grid point requires only the information of the neighboring grid points. Therefore, LETKF offers outstanding scalability properties. SPEEDY-LETKF is an open-source software which have already been widely used for several DA studies (Li et al., 2009; Miyoshi, 2010; Lien et al., 2013; Ruiz et al., 2013; Amezcua et al., 2014). Here, SPEEDY-LETKF was extended for the assimilation of TA linear observations and pseudo-TRW observations. This was done by (i) modification of the model time cycling, (ii) addition of the TA-Up updating approach and (iii) development of the VSL-like observation operator.

For the experiments presented in this paper, we employed ensembles of 24 members (limited by the number of CPUs) and constant multiplicative inflation of 1% after the ensemble update. R-localization (Hunt et al., 2007) is achieved using the following formula:

$$R_{loc} = R * \exp\left(\left(r_h/2\lambda_h\right)^2 + \left(r_v/2\lambda_v\right)^2\right) \quad (8)$$

where  $r_h$  and  $r_v$  stand for the horizontal and vertical distances, respectively. Their corresponding scaling parameters were set to the values  $\lambda_h = 500$  Km and  $\lambda_v = 0.4 \ln p$ . Additionally, in order to avoid catastrophic filter divergence, observations with huge divergence from their corresponding predicted values are neglected. The observation quality control strategy within the SPEEDY-LETKF is as the following: observations whose corresponding innovation vector norm (absolute mismatch regarding the forecast observation) is bigger than 10 times its error standard deviation, are discarded.

### 2.3.3 Runs' characteristics

The modified version of SPEEDY-LETKF is utilized to carry out a set of standard "perfect model" Observation System Simulation Experiments (OSSEs, see Appendix A and Fig. 1) (Errico et al., 2013). The model can be coupled with a shallow ocean which contains a 50 m deep thermodynamic slab ocean layer (Herceg Bulić and Kucharski, 2012). First the VSL-T representation of the PLF is utilized for two sets of experiments under different ocean conditions:

- *PRESCRIBED experiment* is forced by the boundary conditions included in the version 41 of the code, which comprises the sea surface temperature (SST) anomalies from 1854 to 2010 with respect to the period 1979 to 2008 derived from



NOAA\_ERSST\_V3 dataset (Smith et al., 2008; Xue et al., 2003), as well as climatological maps derived from input data of the ECMWF's reanalysis (Gibson et al., 1997). The latter consist of soil wetness, land temperature, snow depth, ice cover, vegetation cover and albedo monthly maps. This procedure follows the AMIP-type experiments (Herceg Bulić and Kucharski, 2012).

- 5 • *SLAB experiment* is coupled with a slab ocean model (“q-flux adjusted mixed layer model”) forced by climatological ocean dynamics and no initialization is used. The model starts from the equilibrium.

Then, for the sake of simplicity and computational affordability, only two representations of the PLF are considered: the “minimum” and the “product” Triangular Norms (t-norms). This selection is based on the results of AC15 experiments.

- 10 Initially, a one-year long spin-up run is performed for all experiments, starting from January 1<sup>st</sup>, 1860. The final state of this model trajectory is subsequently used as initial condition for a 150 years long nature run. The ensemble runs with and without DA are identically initialized from a set of states gathered daily from the last two month of the spin-up run (lagged 2 day initialization). Notice that the nature run and the different ensemble runs are generated driving SPEEDY with the same time varying forcing fields.

## 2.4 Observation generation

- 15 Pseudo-TRW observations are produced following VSL's formulation, plus a final white noise addition step, where random draws from a Gaussian distribution are added to the clean TA observations, so as to obtain a Signal to Noise Ratio (SNR) equal to 10.0. Surface temperature data was extracted from the lowest level of the state vector, while soil moisture was taken from the surface boundary conditions. Notice that temperature is a prognostic variable of the model, whereas soil moisture is a prescribed variable with yearly periodicity. It is worthwhile to mention that although soil moisture is not a prognostic variable  
20 of SPEEDY, it does affect prognostic variables, such as humidity, through the parametrizations.

- Regarding the geographical distribution of observations, we place a station at every grid box where at least one actual TRW chronology from the database of Breitenmoser et al. (2014) is present. This strategy yields an observational network comprising 257 stations (see figure 2). Concerning the configuration of the observation operator, for our experiment involving SPEEDY we focus on the effect of the first VSL's nonlinearity, i.e., the shifting of recorded variable. Consequently, we configure VSL so  
25 that no thresholding takes place. This is done by setting the upper and lower response thresholds to the maximum and minimum values during the nature run, respectively, so that the response functions reduce to linear rescaling operators (ref. AC15).

## 2.5 Diagnostic statistics

- Given the annual resolution of TRW chronologies, we study the filter performance for a fixed averaging period length of one year. We monitor the behavior of ensemble runs by means of Root Mean Square Error (RMSE) for the near surface Temperature  
30 (see Appendix A). SPEEDY presents spatially heterogeneous internal variability. Due to this feature, for a particular time averaging length, there will typically be regions with very low internal variability (eg., equatorial regions for temperature) for which RMSE shows very low values.



The results are illustrated by three kinds of presentations: 1) time-series of globally averaged temperature RMSE, 2) histograms of these time-series and 3) maps of time-averaged (150 years) temperature RMSEs. We note that the selection of temperature variable is due to its larger error reduction compared to other variables (*eg*, humidity, u-wind, v-wind) when DA is applied.

## 5 3 Results

### 3.1 Free ensemble run

An AGCM is an example of non-autonomous system and accordingly the evolution of its state is determined by both the atmospheric dynamics and the external forcing. The influences of these two distinct factors can be disentangle to a good extend by considering the atmospheric variability as a linear superposition of an internal component, caused by the intrinsic dynamics, and an external one, resulting from the variations of the boundary conditions (Deza et al., 2014). Under this assumption, internal and external variability can be separated by way of a free ensemble run, using the ensemble mean as an estimate of the forced component. The magnitude of the internal variability can then be estimated from the ensemble spread. Note that using an ensemble DA method is only beneficial in the presence of internal variability, given that the forced variability can be well described by an unconstrained ensemble run.

#### 15 3.1.1 Free ensemble spread and error

The time averaging operator acts as a low pass filter that reduces the amplitude of fluctuations with time scales shorter than the averaging period. Subsequently, geographical areas dominated by fast processes, compared to averaging period ( $\tau_{aver}$ ), tend to present constant mean values, or equivalently no internal time averaged variability. The climatology and the formulation of the SPEEDY model is fully described in Molteni (2003b). Therefore, we focus only on the results of the DA approach, without considering the systematic errors of the model. In the case of TRW chronologies, the characteristic one-year averaging period is long for atmospheric phenomena, and as consequence several areas show very low yearly internal variability for certain variables. A clear example of this is temperature around the equator (see figure 3.a) where the temperature variability is dominated by the daily cycle and accordingly is strongly attenuated by the yearly averaging. On the other hand, planetary scale patterns are not completely stationary but present fluctuations over long time scales. These slow processes introduce internal variability in the yearly means, as can be seen in figure 3.a. Maximum temperature spread occur near the surface at high latitudes around  $\pm 70^\circ$ . These yearly internal variability maxima can be related to leading variability modes of the global circulation, such as the “annular modes” (Thompson and Wallace, 2000), migrations of the ITCZ (Schneider et al., 2014), as well as jet stream displacements (Woollings et al., 2011).

An important consequence of the spatially heterogeneous yearly internal variability of SPEEDY, is that the nature run variables at geographical areas with low internal variability can be well predicted by the ensemble mean of the free ensemble run, as it can be seen in figure 3.b for the tropical surface temperature. On the other hand, RMSE extremes take place in areas of





maximal internal variability (compare figures 3.a and 3.b). Generally, the error of the free ensemble run, used as a predictor of the nature run, is essentially the projection of the nature run trajectory on the internal variability component. Figure 3 exhibits the results for the SLAB experiment and the PRESCRIBED experiment presents very similar behavior.

### 3.2 Assimilating pseudo-TRW observations

#### 5 3.2.1 Temperature-based PLF representation (VSL-T)

As described in Sec. 2.3.3, we investigate two different experiments using SLAB and PRESCRIBED ocean conditions (see Table 1). For the sake of simplicity, we set up the sensitivity experiments using the simple observation operator VSL-T to investigate the effect of the SLAB ocean model. The use of SLAB ocean is motivated by the fact that the coupled ocean may lend predictability to the atmosphere as a slow component of the climate system. On the other hand, the climate of the PRESCRIBED experiment may follow the trends of the forced ocean conditions instead of the terrestrial proxy records. Therefore, the PRESCRIBED experiment's spread and error are expected to be smaller than the SLAB experiment. Figure 4 supports this hypothesis, showing a reduction in globally averaged free ensemble error in PRESCRIBED compared with the SLAB.

Figure 4.a illustrates that no error reduction is obtained for the forecasted temperatures. The expected value of the RMSE is slightly larger than the free ensemble simulation for both SLAB and PRESCRIBED. However, there exist a DA skill for the *analysis* (Fig. 4.b), especially prior to 1950s. The existence of the trend in the RMSE time-series may arise from cycling (reinitialization) of the ensemble or the choice of observation operator (more details in Sec. 4.2). The distribution density of the proxy records' location is biased to the Northern hemisphere, therefore, the error reduction of the *analysis* is more evident in the RMSE maps (Fig. 5).

An important aspect of our results concerning the DA skill, when yearly averaged linear observations are assimilated, is that the error reduction regarding the free ensemble run appears modulated by the magnitude of the yearly internal variability of the particular variable at a specific site (compare figures 4 and 5). As a consequence, stations located in areas of strong yearly internal variability are more efficient than the others at reducing the error of the TA state estimate. An example of this are the stations located in Alaska which constrain temperature considerably more strongly than the ones laying on south Africa. This finding can then be utilized as guidance for the design of optimal TRW chronology networks, in particular, and proxy networks in general (see the discussion at the end of this paper).

This situation, where a DA method presents TA *analysis* skill for averaging periods where the TA *forecast* skill is completely lost, has been previously observed in studies applying EnKF techniques on TA quantities (Bhend et al., 2012; Huntley and Hakim, 2010; Steiger et al., 2014; Pendergrass et al., 2012). DA performed under these circumstances is currently labeled as "off-line". This term is used to indicate that, under the randomizing action of chaotic model dynamics, at assimilation time, the prior ensemble is completely decorrelated from the previous *analysis* state. As a consequence, the observational information cannot accumulate over time, as opposed to the typical application of DA for short-range prediction. This complete absence of observational constraint on the *forecast* implies that our DA experiments are performed in an "off-line" regime.





### 3.2.2 Original and Product PLF representation (VSL-Min and VSL-Prod)

#### 3.2.2.1 DA with cycling

Considering the SLAB experiment, we compare the two nonlinear PLF representations in our DA setting (VSL-Min and VSL-Prod). As illustrated in figure 6.a, the DA *forecast* presents no skill in the globally averaged temperature for both of the  
5 representations. However, the use of VSL-Prod, instead of VSL-Min, as TRW observation operator appears beneficial to the filter performance for the *analysis* as it can be seen in figure 6.b. The expected value of the RMSE presents a significant shift towards lower values for VSL-Prod compared to the free ensemble run. Similar to the case of VSL-T, the RMSE time-series present an increasing trend for both VSL-Min and VSL-Prod.

The RMSEs of DA *forecasts* using different VSL representations (figures 5.a, 7.a and 8.a) do not indicate any improvement  
10 over the free ensemble run (Fig. 3.b). The *analysis* of VSL-Prod performs a slightly better skill than VSL-Min over Europe, the United States and Central Asia. Due to the strong nonlinear features of VSL-Min and VSL-Prod, the performance of these filters is expected to be degraded with respect to the ensemble runs constrained with VSL-T linear observation (see AC15). This behavior can be readily seen by comparing the figures 5.b, 7.b and 8.b.

#### 3.2.2.2 DA with no-cycling

15 Our experiments show that the DA *forecast* has no skill over the model climatology. Therefore, we investigate the idea of purely “off-line” DA. The free ensemble simulation at any individual year is used as the prior state vector for that year instead of the DA *forecast*. Following this methodology, the cycling step (reinitialization) of the ensemble is neglected and the TA DA technique is applied parallel and independent at any specific year of the free ensemble run.

A very interesting feature of figure 9 is that the increasing trends in the RMSE time-series of the *analysis* have vanished. This  
20 indicates that the previously existing trends in the *forecast* and consequently in the *analysis* originated from the reinitialization step of the system but not the proxy records. Figure 10 also confirms that the performance of no-cycling DA can compete with the performance of the online DA.

## 4 Discussion and Outlook

### 4.1 Error reduction efficacy of TRW chronologies

25 For the OSSE studied here, it was found that the ability of a particular pseudo-TRW chronology to reduce the error of the EnKF-based estimate of the TA state appears modulated by the strength of the yearly internal variability of the model at the chronology site. This finding can in principle be employed to help the dendrochronology community to increase the effectivity of their sampling efforts by focusing on the sites with more potential to decrease reconstruction uncertainty. Furthermore, this approach can be directly applied to any proxy type with sufficiently stable time resolution.



An evident caveat of the above mentioned rationale is that every model-based estimate of the climate internal variability strength for a particular time scale will necessarily exhibit the biases of the particular climate model used. We consider that this modeling subjectivity/imperfection issue can be ameliorated by means of multi-model and multi-physics approaches, which in principle should increase the robustness of the results and provide uncertainty estimates. In any case, we believe that provided, the results are analyzed cautiously taking into account the weaknesses of current climate models, the huge amount of climate dynamics knowledge condensed into an Earth system model can certainly be used profitably to reduce the cost of a indiscriminated proxy sampling strategy.

## 4.2 Off-line regime

Additional to the classical DA approaches used in the paleoclimate studies, a so-called “off-line” DA-based climate reconstructions is presented by (Steiger et al., 2014; Hakim et al., 2016). In their novel method, the same prior or background ensemble is used for each reconstruction time-step. Matsikaris et al. (2015) compared an off-line and an on-line ensemble-based DA and showed that the both methods outperform the model without DA. They concluded that the on-line method performs a more consistence temporal variability. However, they suggested further investigations to evaluate their results.

Within our simplified perfect model OSSE, the observed situation of simultaneously having significant DA skill for *analysis* quantities and none for *forecast* quantities, currently referred to as off-line DA regime, can arise either from the dynamical model or from the DA scheme (answers to the questions 1 and 2 raised in Introduction).

Regarding the dynamical model, the most obvious reason to enter into the off-line regime is that the period between consecutive observations exceeds the predictability horizon of the model. In this conditions, as already discussed in AC15, the ensemble spread reaches climatological levels before new observations are assimilated and the accumulation of observational information is essentially lost. For SPEEDY model, due to its purely atmospheric nature, it is not surprising to enter the off-line regime for a 1-year inter-observation period. This might be also the case for current operational (coupled) climate prediction systems, given their lack of useful lead times longer than one year. In this state of affairs it looks unlikely to achieve effective observational constraint on the *forecast* using proxy records with yearly time resolution. However, there is already evidence for the existence of potential sources of climate internal variability with time scales longer than 1 year (Smith et al., 2012). Accordingly, it is expected to obtain actual inter-annual predictability skills in the foreseeable future.

Regarding the DA scheme, a possible culprit for the onset of the off-line regime is the Time-Averaged Update (TA-Up) strategy (AC15). It is not clear if for SPEEDY model this technique is able to properly estimate instantaneous quantities out of TA observations. In particular complete decorrelation between time averaged and instantaneous variables is not guaranteed.

In any case, despite its lack of accumulation of observational information over time, off-line DA has already been shown to be more robust than traditional CFR techniques based on orthogonal empirical functions (Steiger et al., 2014; Hakim et al., 2016). Moreover, the implementation and running of offline DA schemes is remarkably cheaper than on-line approaches.

Following the idea of (Steiger et al., 2014; Matsikaris et al., 2015; Hakim et al., 2016) for purely “offline” DA (no-cycling), our perfect model experiments indicate that the “online” scheme may not outperform the “offline” one in either the temporal or the spatial error reduction (answer to the question 3 raised in Introduction). It should also be emphasized that our model



set-up (with slab ocean) can not capture the fully atmosphere-ocean interactions. Therefore, using a more realistic coupled atmosphere-ocean model may improve the skill of the “online” DA.

### 4.3 Filter operation sensitivity to the PLF representation

The results of the DA experiments conducted with speedy model support in general the ones obtained for the two-scale Lorenz (1996) model (AC15) regarding the influence of the PLF representation on the filter performance. The efficacy of the EnKF-based TA state estimation strategy appeared to be significantly sensitive to the selection of the t-norm used to calculate the growth rate, with the product t-norm (VSL-Prod) outperforming the minimum t-norm (VSL-Min) used in the original formulation of VSL forward model.

Tolwinski-Ward et al. (2014) described trees as fundamentally lossy<sup>1</sup> recorders of climate, due to the integrated nature of the information in them contained and the standardization process used to minimize the non-climatic effects on growth. In the same vein, we argue that the abrupt shifting of recorded variable –implied by the minimum function used in VSL’s original formulation– might constitute an additional source of lossiness (at least within a EnKF-based DA setting used), which can be substantially reduced by resorting to alternative FL-based representations of the PLF. Our DA experiment indicates a higher skill performance with the VSL-Prod for both “offline” and “online” regimes compared to the VSL-Min (answer to the question 4 raised in Introduction).

### 4.4 Challenges to be addressed

As a cautionary remark, we want to highlight the several important limitations of the experiments described in this paper. The generated pseudo-TRW observations lack response saturation and their contamination with noise was performed assuming optimistically high SNR levels. Furthermore, the response thresholds were set in a completely homogeneous fashion for all the observational stations, whereas actual TRW networks are strongly heterogeneous in that sense, comprising chronologies generated under highly dissimilar growth limitation regimes. Additionally, the efficiency of EnKF technique used relies on the Gaussianity of all the variables of the model. Nevertheless, in a climate model some variables can present strongly non-Gaussian properties –specially definite positive quantities such as humidity– and then their estimation should in principle be performed with more sophisticated strategies such a Gaussian anamorphosis (Bocquet et al., 2010; Lien et al., 2013). It is worth mentioning the necessity of explicitly addressing model errors by conducting imperfect model OSSE. Finally, we note that our findings are based on a slab coupled ocean model and we encourage using a proper coupled atmosphere-ocean model in future studies.

---

<sup>1</sup>This adjective is currently used in the information technology area to designate data encoding methods that lead to information loss from the original version for the sake of reducing the amount of data needed to store the content.



## A Appendix: Observation System Simulation Experiments (OSSE)

Given a prediction system comprising a dynamical model and a DA scheme, *forecast* and *analysis* errors arise from many different sources, e.g. model imperfections, inadequacy of the DA strategy and insufficiency of observational information, which interact with each other in practice. In order to disentangle the effects of these error sources, a DA scheme is typically tested under simplified conditions by means of numerical experiments, currently known as OSSE, whose realism level is gradually increased.

An OSSE consists of (i) a single model trajectory  $\mathbf{x}^{\text{NATURE}}$ , typically referred to as “true” run or “nature” run, that is used as prediction target, (ii) pseudo-observations created by applying the observation operator to  $\mathbf{x}^{\text{NATURE}}$  and adding simulated observational noise, and (iii) an observationally constrained run  $\mathbf{X}^{\text{DA}}$ , obtained by performing a sequence of *analysis* cycles where the pseudo-observations are assimilated (see Fig. 1).

The nature run is normally generated by running the dynamical model starting from a random sample of the model climatology. Notice that thanks to the availability of the truth model evolution for an OSSE, the *forecast* and *analysis* skill of the observationally constrained run can be directly assessed, using for example the RMSE of the ensemble mean:

$$\text{RMSE}(\langle \mathbf{X}^{\text{DA}} \rangle) = \left( \overline{(\mathbf{x}^{\text{NATURE}} - \langle \mathbf{X}^{\text{DA}} \rangle)^2} \right)^{\frac{1}{2}}, \quad (\text{A1})$$

where  $\overline{\quad}$  and  $\langle \quad \rangle$  denote the time and ensemble mean operators, respectively.

An additional run frequently performed for OSSE involving ensemble DA methods, is a free ensemble run  $\mathbf{X}^{\text{FREE}}$ , where no observations are assimilated and then the ensemble just freely evolved under the action of the model dynamics.  $\mathbf{X}^{\text{FREE}}$  is intended to provide a benchmark of performance, against which it is possible to assess the added value of the DA scheme. As mentioned before, the development and evaluation of a DA setting should be carried out gradually, by way of a hierarchy of increasingly realistic OSSE. A typical first step is to create  $\mathbf{x}^{\text{NATURE}}$ ,  $\mathbf{X}^{\text{FREE}}$  and  $\mathbf{X}^{\text{DA}}$  using the same model, which leads to the so-called “perfect model” OSSE. In a real-world setting the dynamical model is always an imperfect representation of reality, then a natural next step is a “imperfect model” OSSE, where  $\mathbf{X}^{\text{FREE}}$  and  $\mathbf{X}^{\text{DA}}$  are performed using for example a simplified version of the model utilized to create  $\mathbf{x}^{\text{NATURE}}$ .

*Acknowledgements.* The computational resources were made available by the High Performance Computing Center (ZEDAT) at Freie Universität Berlin and the German Climate Computing Center (DKRZ). This work was supported by German Federal Ministry of Education and Research (BMBF) as Research for Sustainability initiative (FONA); www.fona.de through Palmod project (FKZ: 01LP1511A). W.A. wishes to acknowledge partial financial support by the Helmholtz graduate research school GEOSIM.



## References

- Acevedo, W., Reich, S., and Cubasch, U.: Towards the assimilation of tree-ring-width records using ensemble Kalman filtering techniques, *Climate Dynamics*, pp. 1–12–, <http://dx.doi.org/10.1007/s00382-015-2683-1>, 2015.
- Amezcu, J., Ide, K., Kalnay, E., and Reich, S.: Ensemble transform Kalman-Bucy filters, *Q.J.R. Meteorol. Soc.*, 140, 995–1004, <http://dx.doi.org/10.1002/qj.2186>, 2014.
- 5 Annan, J. D. and Hargreaves, J. C.: Identification of climatic state with limited proxy data, *Clim. Past*, 8, 1141–1151, <http://www.clim-past.net/8/1141/2012/>, 2012.
- Barkmeijer, J., Iversen, T., and Palmer, T. N.: Forcing singular vectors and other sensitive model structures, *Quarterly Journal of the Royal Meteorological Society*, 129, 2401–2423, doi:10.1256/qj.02.126, <http://dx.doi.org/10.1256/qj.02.126>, 2003.
- 10 Bhend, J., Franke, J., Folini, D., Wild, M., and Brönnimann, S.: An ensemble-based approach to climate reconstructions, *Clim. Past*, 8, 963–976, <http://www.clim-past.net/8/963/2012/>, 2012.
- Bocquet, M., Pires, C. A., and Wu, L.: Beyond Gaussian Statistical Modeling in Geophysical Data Assimilation, *Mon. Wea. Rev.*, 138, 2997–3023, <http://dx.doi.org/10.1175/2010MWR3164.1>, 2010.
- Bourke, W.: A Multi-Level Spectral Model. I. Formulation and Hemispheric Integrations, *Mon. Wea. Rev.*, 102, 687–701, [http://dx.doi.org/10.1175/1520-0493\(1974\)102<0687:AMLSMI>2.0.CO;2](http://dx.doi.org/10.1175/1520-0493(1974)102<0687:AMLSMI>2.0.CO;2), 1974.
- 15 Breitenmoser, P., Brönnimann, S., and Frank, D.: Forward modelling of tree-ring width and comparison with a global network of tree-ring chronologies, *Clim. Past*, 10, 437–449, <http://www.clim-past.net/10/437/2014/>, 2014.
- Brönnimann, S.: Towards a paleoreanalysis?, *ProClim-Flash*, 1, 16, 2011.
- Brönnimann, S., Franke, J., Breitenmoser, P., Hakim, G., Goosse, H., Widmann, M., Crucifix, M., Gebbie, G., Annan, J., and van der Schrier, G.: Transient state estimation in paleoclimatology using data assimilation, *PAGES*, 21, 2013.
- 20 Burgers, G., van Leeuwen, P. J., and Evensen, G.: Analysis scheme in the ensemble Kalman filter, *Monthly Weather Review*, 126, 1719–1724, <http://dx.doi.org/10.1029/94JC00572>, 1998.
- Crucifix, M.: Traditional and novel approaches to palaeoclimate modelling, *Quaternary Science Reviews*, 57, 1–16, <http://www.sciencedirect.com/science/article/pii/S0277379112003472>, 2012.
- 25 Deza, J. I., Masoller, C., and Barreiro, M.: Distinguishing the effects of internal and forced atmospheric variability in climate networks, *Nonlin. Processes Geophys.*, 21, 617–631, <http://www.nonlin-processes-geophys.net/21/617/2014/>, 2014.
- Dirren, S. and Hakim, G. J.: Toward the assimilation of time-averaged observations, *Geophysical Research Letters*, 32, L04 804, doi:10.1029/2004GL021444, <http://dx.doi.org/10.1029/2004GL021444>, 2005.
- Dubinkina, S. and Goosse, H.: An assessment of particle filtering methods and nudging for climate state reconstructions, *Climate of the Past*, 9, 1141–1152, doi:10.5194/cp-9-1141-2013, <http://www.clim-past.net/9/1141/2013/>, 2013.
- 30 Dubinkina, S., Goosse, H., Sallaz-Damaz, Y., Crespin, E., and Crucifix, M.: Testing a particle filter to reconstruction climate over the past centuries, *Int. J. Bifurcation Chaos*, 21, 3611–3618, doi:10.1142/S0218127411030763, <http://dx.doi.org/10.1142/S0218127411030763>, 2011.
- Errico, R. M., Yang, R., Privé, N. C., Tai, K.-S., Todling, R., Sienkiewicz, M. E., and Guo, J.: Development and validation of observing-system simulation experiments at NASA's Global Modeling and Assimilation Office, *Q.J.R. Meteorol. Soc.*, 139, 1162–1178, <http://dx.doi.org/10.1002/qj.2027>, 2013.
- 35



- Evans, M., Tolwinski-Ward, S., Thompson, D., and Anchukaitis, K.: Applications of proxy system modeling in high resolution paleoclimatology, *Quaternary Science Reviews*, 76, 16 – 28, doi:<http://dx.doi.org/10.1016/j.quascirev.2013.05.024>, <http://www.sciencedirect.com/science/article/pii/S0277379113002011>, 2013.
- Evensen, G.: The Ensemble Kalman Filter: theoretical formulation and practical implementation, *Ocean Dynamics*, 53, 343–367, <http://dx.doi.org/10.1007/s10236-003-0036-9>, 2003.
- Gibson, J. K., Källberg, P., Uppala, S., Nomura, A., Hernandez, A., and Serrano, E.: ERA Description, in: ECMWF ERA-15 Project Report Series, No. 1, European Centre for Medium-Range Weather Forecasts, Shinfield, Reading, UK, 1997.
- Hakim, G., Annan, J., Broennimann, S., Crucifix, M., Edwards, T., Goosse, H., Paul, A., van der Schrier, G., and Widmann, M.: Overview of data assimilation methods, *PAGES*, 21, 2013.
- Hakim, G. J., Emile-Geay, J., Steig, E. J., Noone, D., Anderson, D. M., Tardif, R., Steiger, N., and Perkins, W. A.: The last millennium climate reanalysis project: Framework and first results, *J. Geophys. Res. Atmos.*, 121, 6745–6764, <http://dx.doi.org/10.1002/2016JD024751>, 2016.
- Hamill, T. M.: Ensemble-based atmospheric data assimilation, in: *Predictability of Weather and Climate*, edited by Palmer, T. and Hagedorn, R., Cambridge University Press, web: <http://dx.doi.org/10.1017/CBO9780511617652.007>, 2006.
- Herceg Bulić, I. and Kucharski, F.: Delayed ENSO impact on spring precipitation over North/Atlantic European region, *Climate Dynamics*, 38, 2593–2612, <http://dx.doi.org/10.1007/s00382-011-1151-9>, 2012.
- Hughes, M. and Ammann, C.: The future of the past – an earth system framework for high resolution paleoclimatology: editorial essay, *Climatic Change*, 94, 247–259, doi:10.1007/s10584-009-9588-0, <http://dx.doi.org/10.1007/s10584-009-9588-0>, 2009.
- Hughes, M., Guiot, J., and Ammann, C.: An emerging paradigm: Process-based climate reconstructions, *PAGES news*, 18, 87–89, 2010.
- Hunt, B. R., Kostelich, E. J., and Szunyogh, I.: Efficient data assimilation for spatiotemporal chaos: A local ensemble transform Kalman filter, *Physica D: Nonlinear Phenomena*, 230, 112–126, <http://www.sciencedirect.com/science/article/pii/S0167278906004647>, 2007.
- Huntley, H. and Hakim, G.: Assimilation of time-averaged observations in a quasi-geostrophic atmospheric jet model, 35, 995–1009–, <http://dx.doi.org/10.1007/s00382-009-0714-5>, 2010.
- Kurahashi-Nakamura, T., Losch, M., and Paul, A.: Can sparse proxy data constrain the strength of the Atlantic meridional overturning circulation?, *Geoscientific Model Development*, 7, 419–432, doi:10.5194/gmd-7-419-2014, <http://www.geosci-model-dev.net/7/419/2014/>, 2014.
- Li, H., Kalnay, E., Miyoshi, T., and Danforth, C. M.: Accounting for Model Errors in Ensemble Data Assimilation, *Mon. Wea. Rev.*, 137, 3407–3419, <http://dx.doi.org/10.1175/2009MWR2766.1>, 2009.
- Lien, G.-Y., Kalnay, E., and Miyoshi, T.: Effective assimilation of global precipitation: simulation experiments, 2013, 65, <http://www.tellusa.net/index.php/tellusa/article/view/19915>, 2013.
- Lorenz, E. N.: Predictability, a problem partly solved, in: *Proceedings of ECMWF seminar on Predictability*, pp. 1–19, ECMWF, Reading, UK, 1996.
- Mathiot, P., Goosse, H., Crosta, X., Stenni, B., Braida, M., Renssen, H., Van Meerbeeck, C. J., Masson-Delmotte, V., Mairesse, A., and Dubinkina, S.: Using data assimilation to investigate the causes of Southern Hemisphere high latitude cooling from 10 to 8 ka BP, *Climate of the Past*, 9, 887–901, doi:10.5194/cp-9-887-2013, <http://www.clim-past.net/9/887/2013/>, 2013.
- Matsikaris, A., Widmann, M., and Jungclauss, J.: On-line and off-line data assimilation in palaeoclimatology: a case study, *Clim. Past*, 11, 81–93, <http://www.clim-past.net/11/81/2015/>, 2015.
- Miyoshi, T.: Ensemble Kalman filter experiments with a primitive-equation global model, Ph.D. thesis, University of Maryland, College Park, 197pp., 2005.



- Miyoshi, T.: The Gaussian Approach to Adaptive Covariance Inflation and Its Implementation with the Local Ensemble Transform Kalman Filter, *Mon. Wea. Rev.*, 139, 1519–1535, <http://dx.doi.org/10.1175/2010MWR3570.1>, 2010.
- Molteni, F.: Atmospheric simulations using a GCM with simplified physical parametrizations. I: model climatology and variability in multi-decadal experiments, 20, 175–191–, <http://dx.doi.org/10.1007/s00382-002-0268-2>, 2003a.
- 5 Molteni, F.: Atmospheric simulations using a GCM with simplified physical parametrizations. I: model climatology and variability in multi-decadal experiments, *Climate Dynamics*, 20, 175–191, <http://dx.doi.org/10.1007/s00382-002-0268-2>, 2003b.
- Oke, P. R., Allen, J. S., Miller, R. N., Egbert, G. D., and Kosro, P. M.: Assimilation of surface velocity data into a primitive equation coastal ocean model, *J.-Geophys.-Res.*, 107, 5–1–5–25, <http://dx.doi.org/10.1029/2000JC000511>, 2002.
- Paul, A. and Schäfer-Neth, C.: How to combine sparse proxy data and coupled climate models, *Quaternary Science Reviews*, 24, 1095–1107, <http://www.sciencedirect.com/science/article/pii/S0277379104002239>, 2005.
- 10 Pendergrass, A., Hakim, G., Battisti, D., and Roe, G.: Coupled Air-Mixed Layer Temperature Predictability for Climate Reconstruction, *Journal of Climate*, 25, 459–472, doi:10.1175/2011JCLI4094.1, <http://dx.doi.org/10.1175/2011JCLI4094.1>, 2012.
- Robert, A.: The integration of a low order spectral form of the primitive meteorological equations, *Journal of the Meteorological Society of Japan*, 44, 237–245, 1966.
- 15 Ruiz, J. J., Pulido, M., and Miyoshi, T.: Estimating Model Parameters with Ensemble-Based Data Assimilation: A Review, *Journal of the Meteorological Society of Japan. Ser. II*, 91, 79–99, doi:10.2151/jmsj.2013-201, 2013.
- Schneider, T., Bischoff, T., and Haug, G. H.: Migrations and dynamics of the intertropical convergence zone, *Nature*, 513, 45–53, <http://dx.doi.org/10.1038/nature13636>, 2014.
- Smith, D. M., Scaife, A. A., and Kirtman, B. P.: What is the current state of scientific knowledge with regard to seasonal and decadal forecasting?, *Environmental Research Letters*, 7, 015 602, <http://stacks.iop.org/1748-9326/7/i=1/a=015602>, 2012.
- 20 Smith, T. M., Reynolds, R. W., Peterson, T. C., and Lawrimore, J.: Improvements to NOAA’s Historical Merged Land-Ocean Surface Temperature Analysis (1880–2006), *J. Climate*, 21, 2283–2296, doi:10.1175/2007JCLI2100.1, <http://dx.doi.org/10.1175/2007JCLI2100.1>, 2008.
- Steiger, N., Hakim, G., Steig, E., Battisti, D., and Roe, G.: Assimilation of Time-Averaged Pseudoproxies for Climate Reconstruction, *Journal of Climate*, 27, 426–441, doi:10.1175/JCLI-D-12-00693.1, <http://dx.doi.org/10.1175/2011JCLI4094.1>, 2014.
- 25 Thompson, D. W. J. and Wallace, J. M.: Annular Modes in the Extratropical Circulation. Part I: Month-to-Month Variability, *J. Climate*, 13, 1000–1016, [http://dx.doi.org/10.1175/1520-0442\(2000\)013<1000:AMITEC>2.0.CO;2](http://dx.doi.org/10.1175/1520-0442(2000)013<1000:AMITEC>2.0.CO;2), 2000.
- Tolwinski-Ward, S., Tingley, M., Evans, M., Hughes, M., and Nychka, D.: Probabilistic reconstructions of local temperature and soil moisture from tree-ring data with potentially time-varying climatic response, *Climate Dynamics*, pp. 1–16, doi:10.1007/s00382-014-2139-z, <http://dx.doi.org/10.1007/s00382-014-2139-z>, 2014.
- 30 Tolwinski-Ward, S. E., Evans, M. N., Hughes, M., and Anchukaitis, K. J.: An efficient forward model of the climate controls on interannual variation in tree-ring width, *Climate Dynamics*, 36, 2419–2439, doi:10.1007/s00382-010-0945-5, <http://dx.doi.org/10.1007/s00382-010-0945-5>, 2011.
- Tolwinski-Ward, S. E., Anchukaitis, K. J., and Evans, M. N.: Bayesian parameter estimation and interpretation for an intermediate model of tree-ring width, *Climate of the Past*, 9, 1481–1493, doi:10.5194/cp-9-1481-2013, <http://www.clim-past.net/9/1481/2013/>, 2013.
- 35 van der Schrier, G. and Barkmeijer, J.: Bjerknæs’ hypothesis on the coldness during AD 1790–1820 revisited, *Climate Dynamics*, 25, 537–553–, <http://dx.doi.org/10.1007/s00382-005-0053-0>, 2005.





**Table 1.** Runs' characteristics.

<i>No.</i>	1	2	3	4
<b>Forward Model</b>	VSL-T	VSL-T	VSL-Min	VSL-Prod
<b>Ocean</b>	<i>SLAB</i>	<i>PRESCRIBED</i>	<i>SLAB</i>	<i>SLAB</i>

Simulations are 150 years long.

- von Storch, H., Cubasch, U., González-Ruoco, J., Jones, J., Widmann, M., and Zorita, E.: Combining paleoclimatic evidence and GCMs by means of Data Assimilation Through Upscaling and Nudging (DATUN), Proceedings 28-31. 11th Symposium on global change studies, AMS, Long Beach, CA, USA.9-14/1, pp. 2119–2128, 2000.
- Whitaker, J. S., Compo, G. P., and Thépaut, J.-N.: A Comparison of Variational and Ensemble-Based Data Assimilation Systems for Reanalysis of Sparse Observations, *Mon. Wea. Rev.*, 137, 1991–1999, <http://dx.doi.org/10.1175/2008MWR2781.1>, 2009.
- 5 Widmann, M., Goosse, H., van der Schrier, G., Schnur, R., and Barkmeijer, J.: Using data assimilation to study extratropical Northern Hemisphere climate over the last millennium, *Climate of the Past*, 6, 627–644, doi:10.5194/cp-6-627-2010, <http://www.clim-past.net/6/627/2010/>, 2010.
- Woollings, T., Pinto, J. G., and Santos, J. A.: Dynamical Evolution of North Atlantic Ridges and Poleward Jet Stream Displacements, *J. Atmos. Sci.*, 68, 954–963, <http://dx.doi.org/10.1175/2011JAS3661.1>, 2011.
- 10 Xue, Y., Smith, T. M., and Reynolds, R. W.: Interdecadal Changes of 30-Yr SST Normals during 1871-2000, *J. Climate*, 16, 1601–1612, doi:10.1175/1520-0442(2003)016<1601:ICOYSN>2.0.CO;2, <http://journals.ametsoc.org/doi/abs/10.1175/1520-0442%282003%29016%3C1601%3AICOYSN%3E2.0.CO%3B2>, 2003.

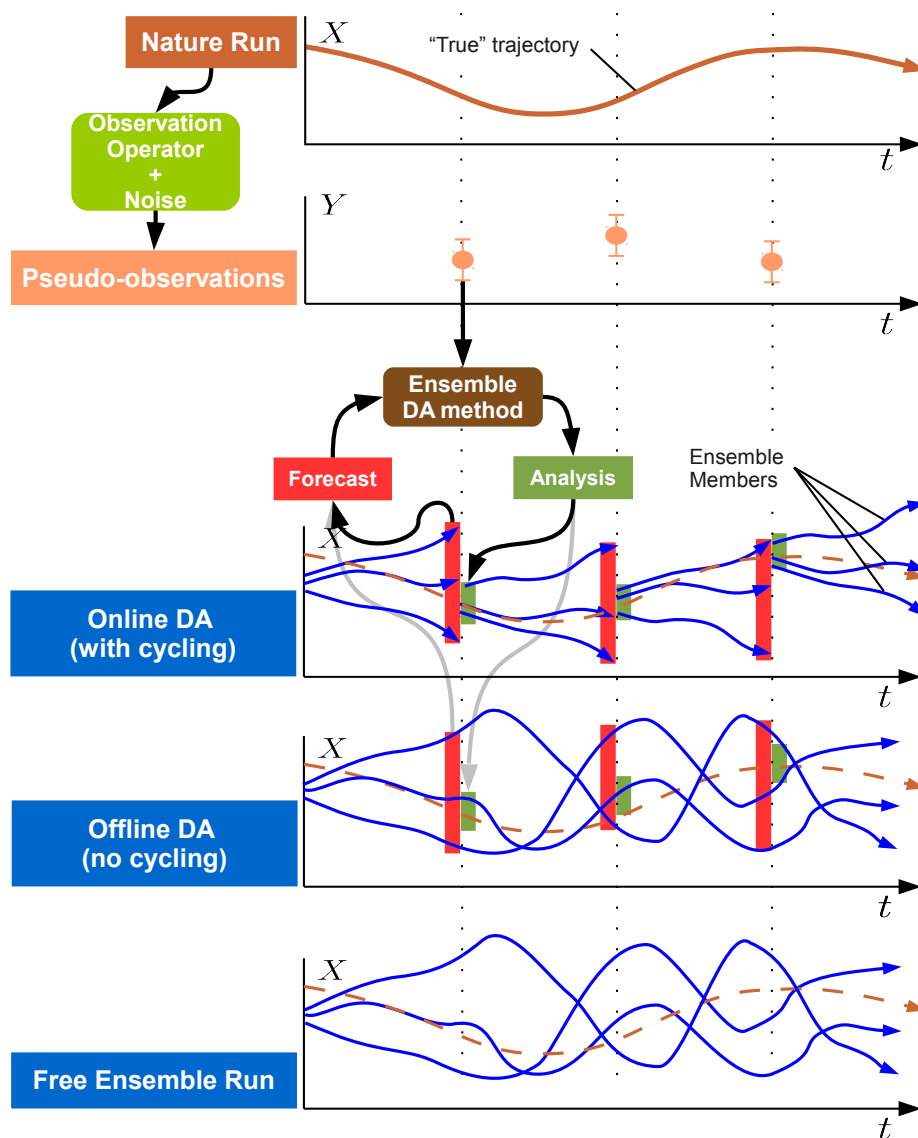


**Figure 1.** Schematic of a typical Observation System Simulation Experiment (OSSE) with ensemble “online” (with cycling) and “offline” (no-cycling) DA methods.  $t$  designates the time axis and  $X(Y)$  denotes the model state (observation) space. Sharp (rounded) cornered boxes represent data (processes). Red (green) vertical shadings indicate the *Forecast (Analysis)* spread. Vertical dotted lines represent the assimilation steps.

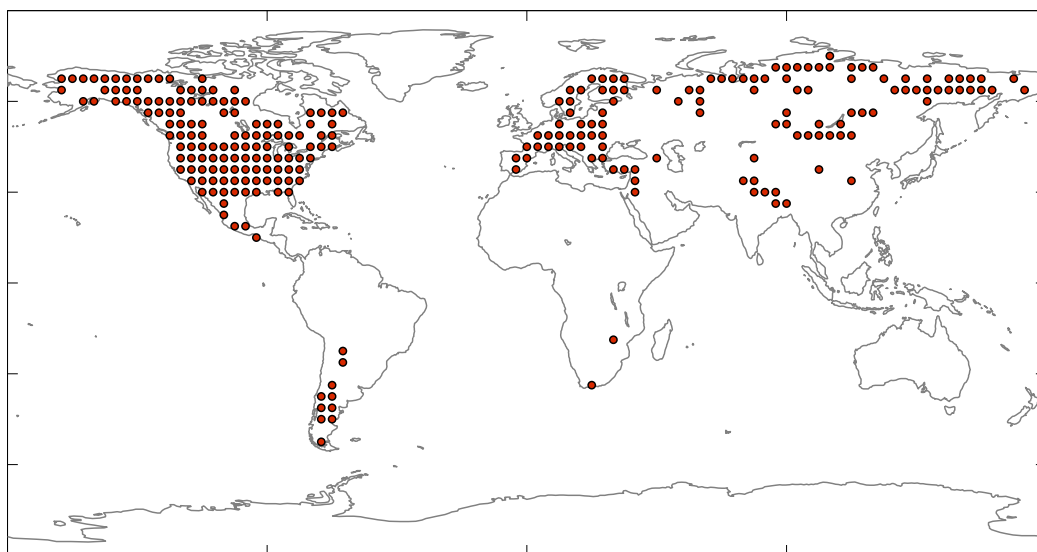
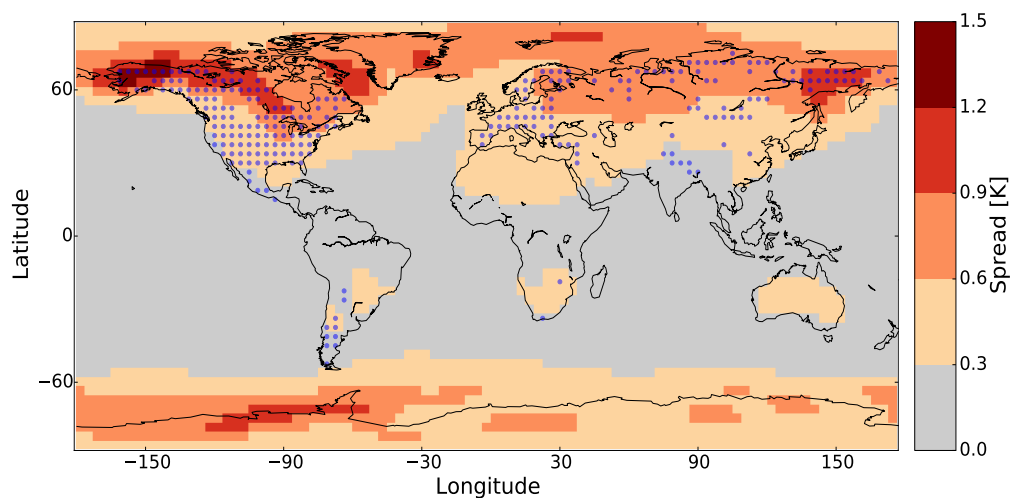


**Figure 2.** Station set resembling real TRW network from Breitenmoser et al. (2014)



**a) Free ensemble Spread**



**b) Free ensemble Error**

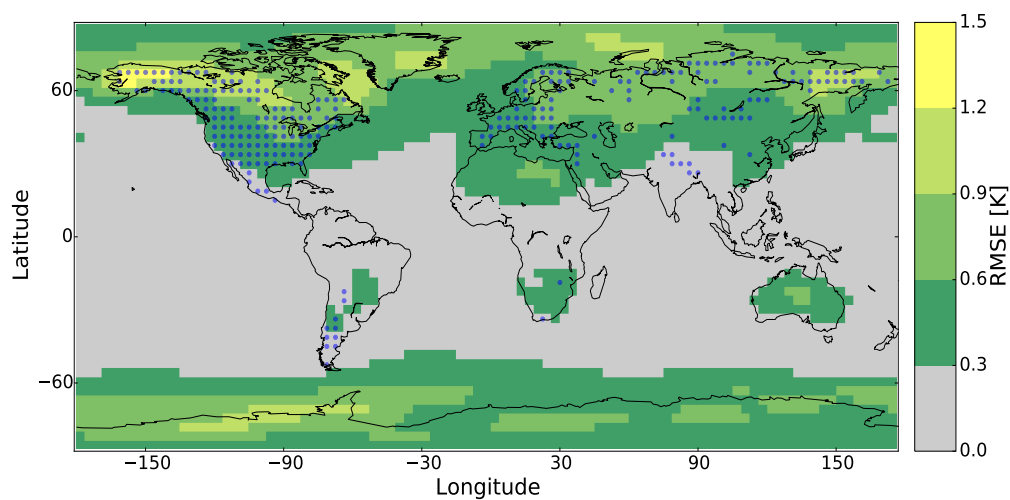


**Figure 3.** Free ensemble simulations for the SLAB experiment: a) Ensemble Spread [K] of near surface temperatures, b) Free ensemble RMSE [K].

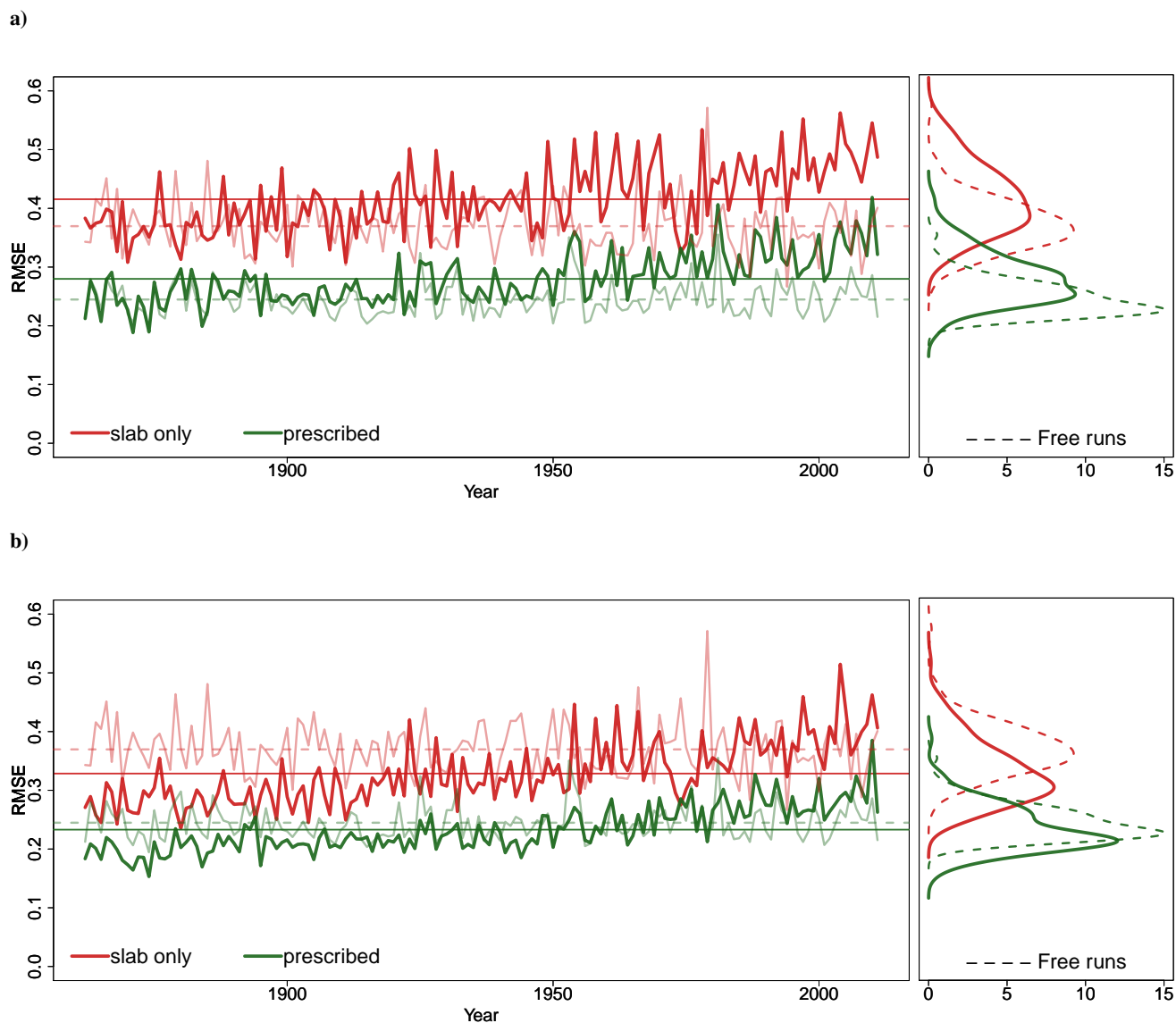
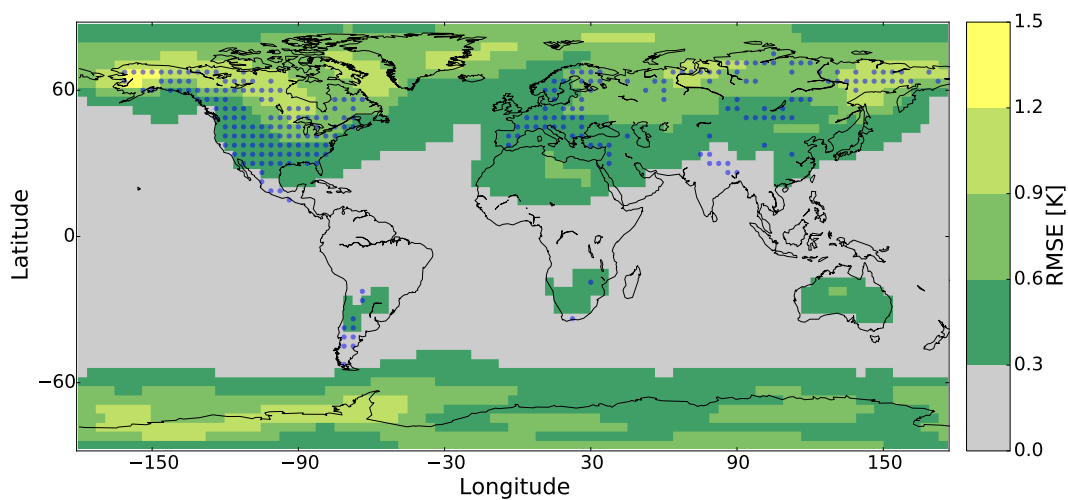


**Figure 4.** Global ensemble mean for a) Forecast constrained by VSL-T pseudo-TRW observations (bold lines) and Free run (thin lines); b) Analysis (solid lines) and Free run (thin lines). Horizontal lines exhibit the mean values. Right panels exhibit the histograms of the time-series.



a) DA forecast for VSL-T



b) DA analysis for VSL-T

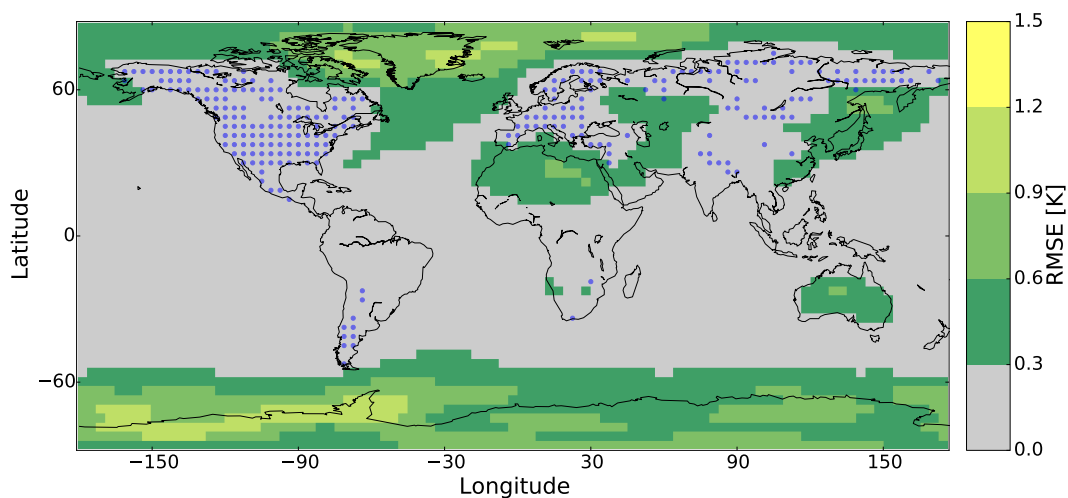


**Figure 5.** Time-averaged RMSEs of SLAB experiment for a) DA *forecast* and b) DA *analysis* using the VSL-T observation operator.

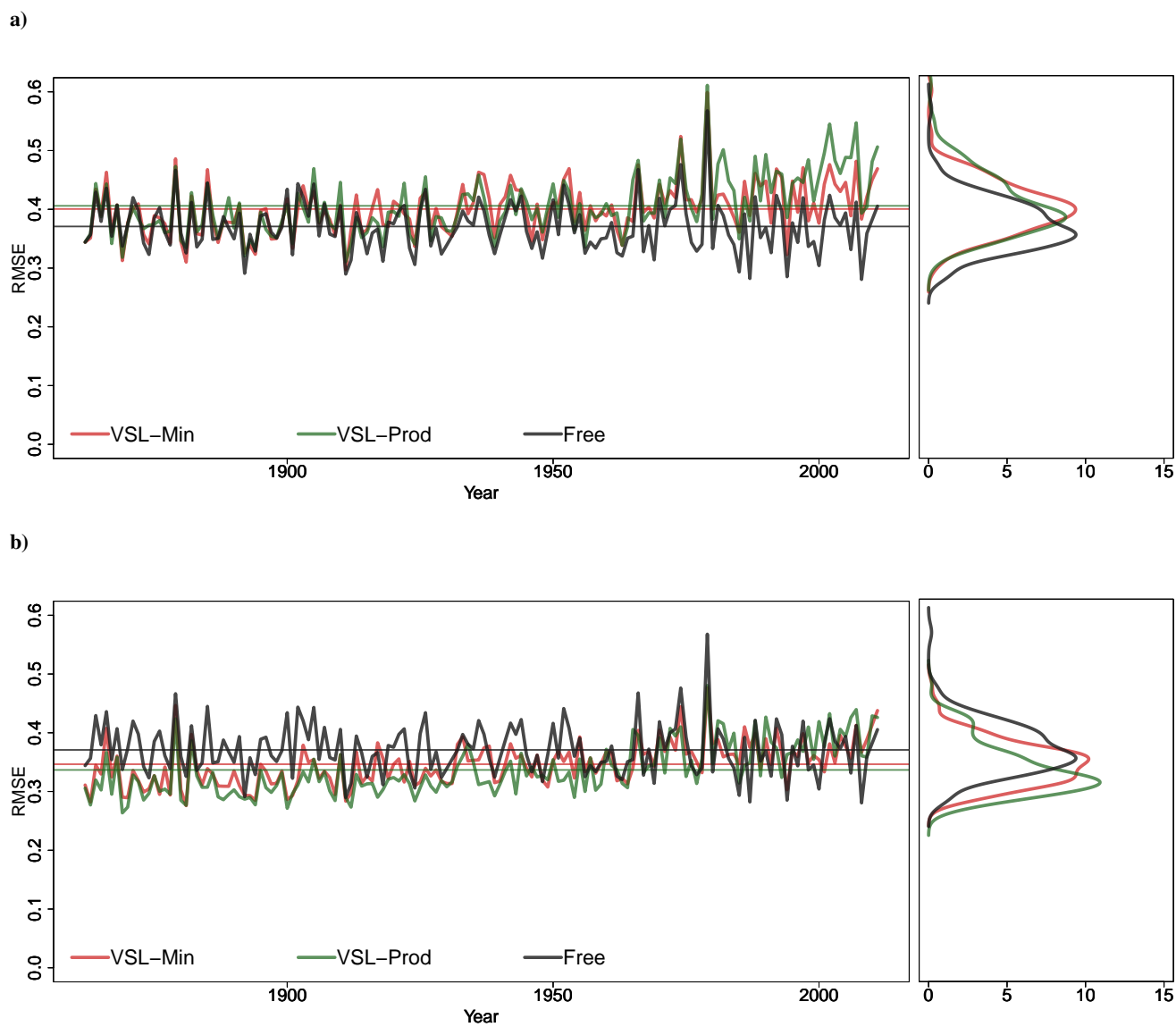
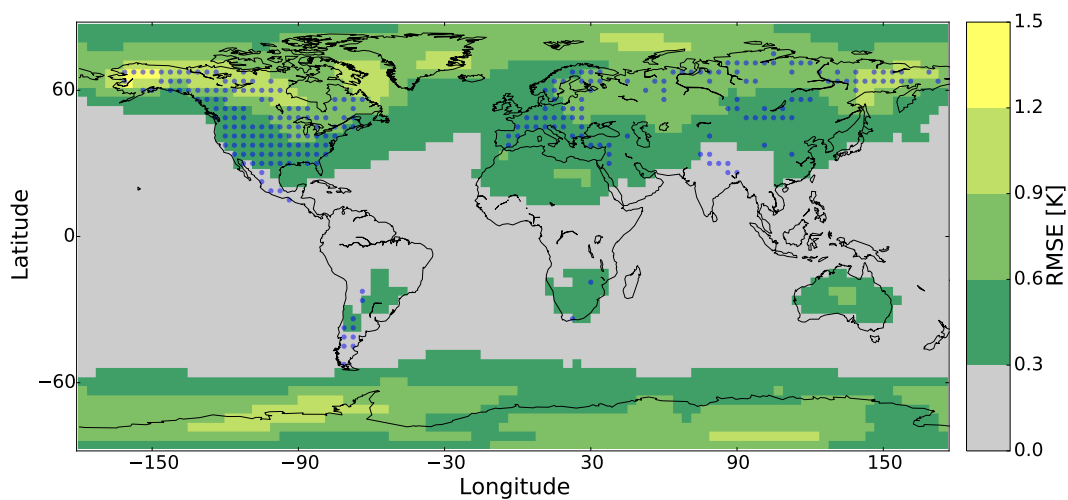


**Figure 6.** Global ensemble mean for a) *forecast* and b) *analysis* constrained by VSL-Min (red) and VSL-Prod (green) pseudo-TRW observations and free run (black). Horizontal lines exhibit the mean values. Right panels exhibit the histograms of the time-series.





a) DA *forecast* for VSL-Min



b) DA *analysis* for VSL-Min

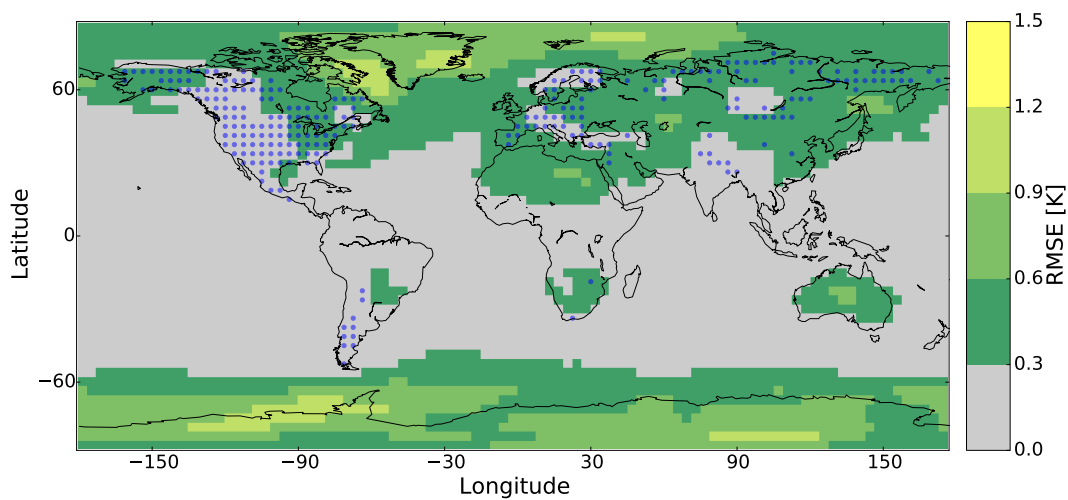
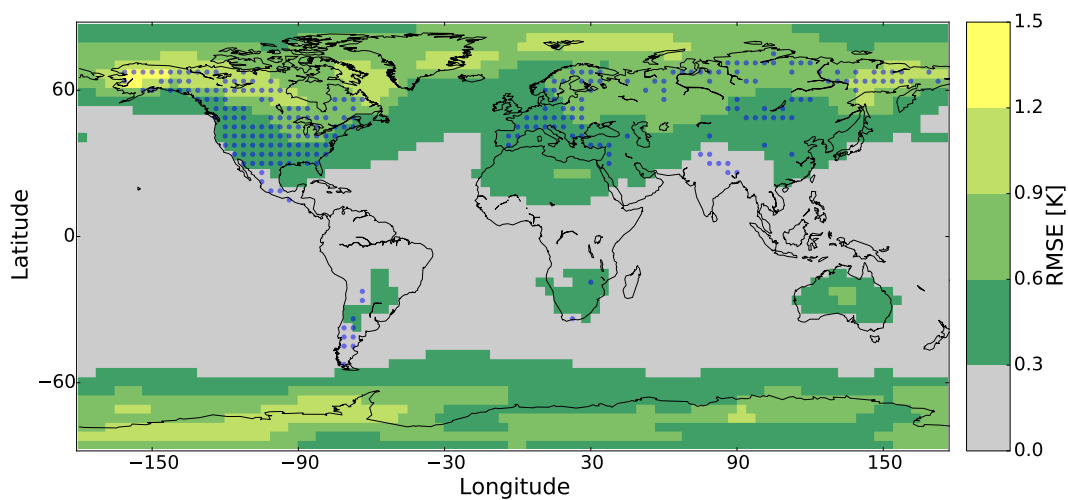


**Figure 7.** Time-averaged RMSEs of SLAB experiment for a) DA *forecast* and b) DA *analysis* using the VSL-Min observation operator.



a) DA *forecast* for VSL-Prod



b) DA *analysis* for VSL-Prod

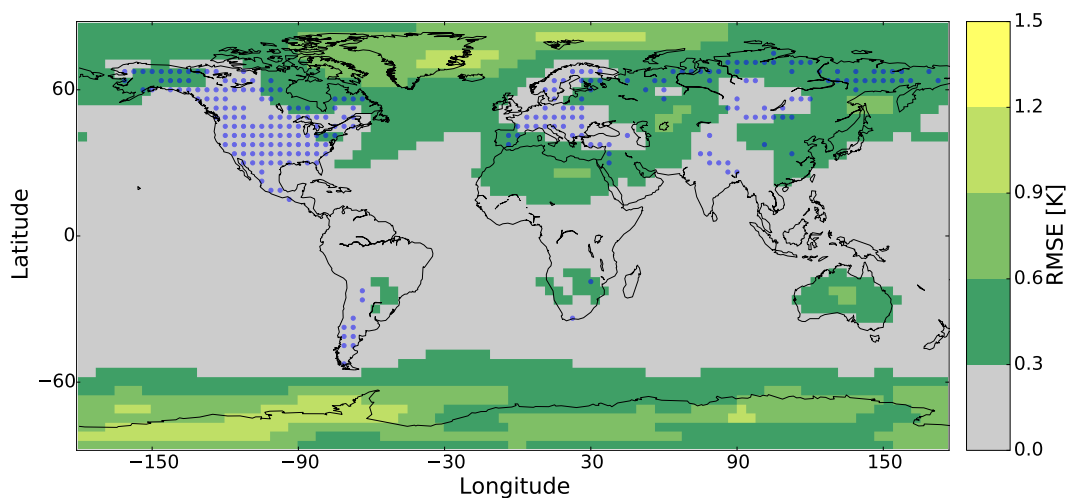


**Figure 8.** Time-averaged RMSEs of SLAB experiment for a) DA *forecast* and b) DA *analysis* using the VSL-Prod observation operator.

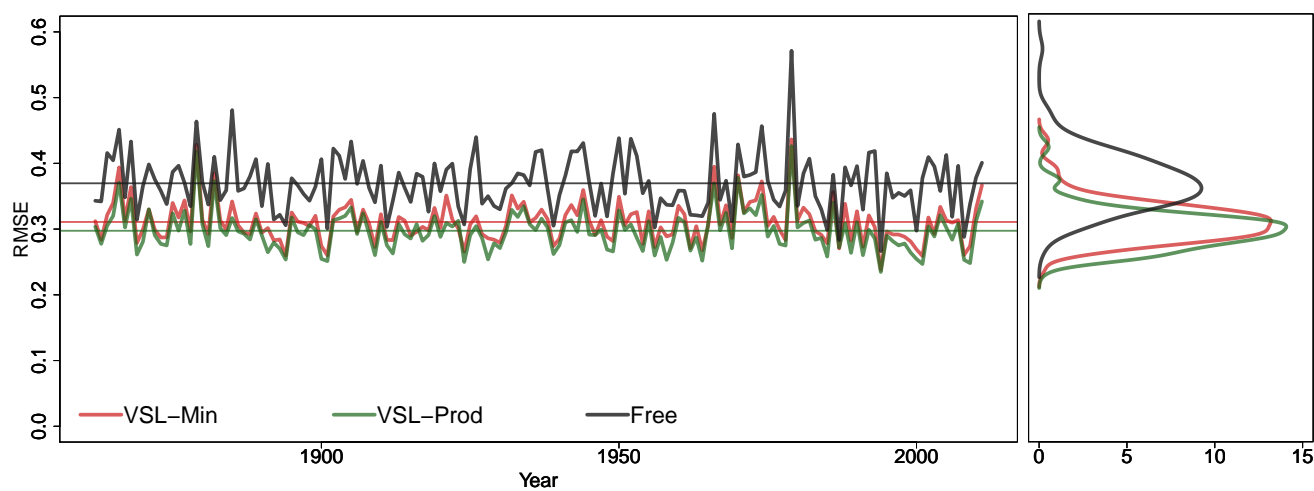
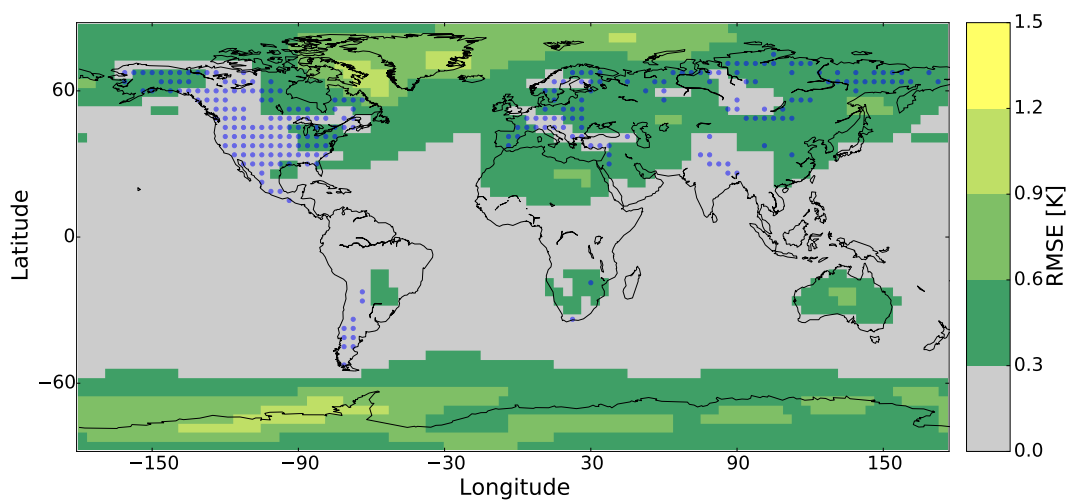


**Figure 9.** Global ensemble mean for *analysis* constrained by VSL-Min (red) and VSL-Prod (green) pseudo-TRW observations and free run (black). Horizontal lines exhibit the mean values. Right panel exhibits the histograms of the time-series.



a) DA analysis for VSL-Min with nocyling



b) DA analysis for VSL-Prod with nocyling

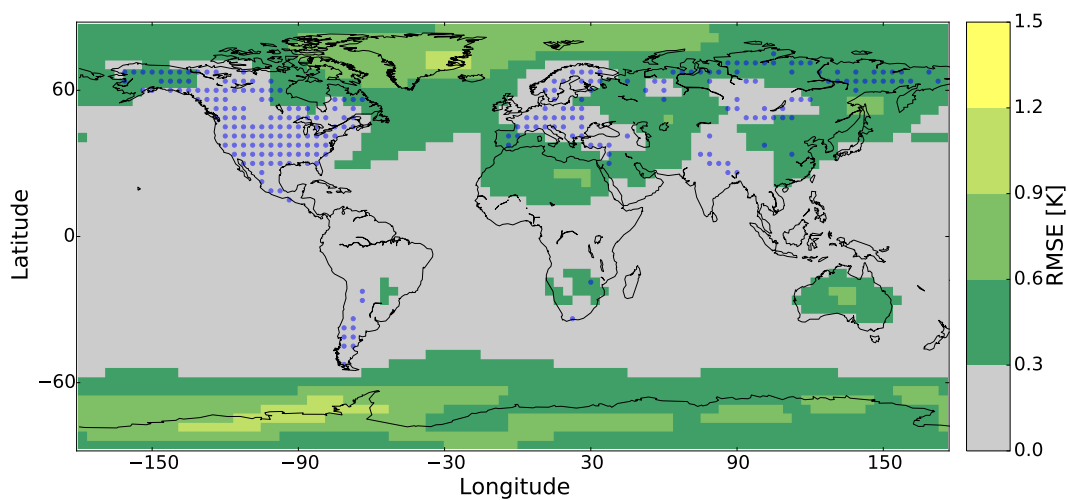


**Figure 10.** Time-averaged RMSEs of SLAB experiment for a) nocyling DA analysis using the VSL-Min and b) the VSL-Prod observation operator.